Synthesis, structural characterization and optical studies of Fe_2O_3 nanoparticles based polymeric materials for flexible electronic devices

B. M. Alotaibi[a], H. A. Al-Yousef[a], A. Atta[b,*], S. A. Rizk[c], A. T. Elgendy[d]
[a]*Department of Physics, College of Science, Princess Nourah bint Abdulrahman University, P.O. Box: 84428, Riyadh 11671, Saudi Arabia*
[b]*Physics Department, College of Science, Jouf University, P.O. Box: 2014, Sakaka, Saudi Arabia*
[c]*Chemistry Department, Science Faculty, Ain Shams University, Cairo, Egypt*
[d]*Physics Department, Science Faculty, Ain Shams University, Cairo, Egypt*

In this work, a thin film containing a flexible polymer nanocomposite of iron oxide (Fe_2O_3) and poly(4-chloroaniline) P(4-ClAni) was successfully synthesized using the green polymerization fabrication method. To confirm the effective synthesis of the P(4-ClAni)/Fe_2O_3 nanocomposite, the XRD, SEM, and FTIR analyses were used. The SEM pictures revealed that the nanocomposite contain Fe_2O_3 nanoparticles distributed throughout the polymer matrix. The optical absorbance of the P(4-ClAni) and P(4-ClAni)/Fe_2O_3 films was measured at room temperature using a UV-vis spectrophotometer from 190 to 1150 nm. The optical properties of P(4-ClAni)/Fe_2O_3 films were calculated using Tauc's relation. The Urbach energy of the P(4-ClAni) increases from 0.96 eV to 1.65 eV, 1.73 eV, and 1.86 eV, respectively, when mixed with 2%, 4%, and 6% of Fe_2O_3. On the other hand, the band gap energy of P(4-ClAni) decreases from 3.57 eV to 3.39 eV, 3.07 eV, and 2.84 eV, respectively, with the addition of 2%, 4%, and 6% Fe_2O_3. Based on the results of this study, the composite P(4-ClAni)/Fe_2O_3 sheets can be used for flexible electronic devices.

(Received March 18, 2024; Accepted June 21, 2024)

*Keywords: Green s*ynthesis, Characterization, Nanocomposites, Optical properties, *Electronic devices.*

1. Introduction

The exceptional properties of polymer nanocomposites, attributed to the inclusion of nanosized fillers, render them highly attractive for use in batteries and electronic devices [1, 2]. These composites pave the way for flexible electronics with better thermal management, allowing for more powerful devices in the electronics industry [3]. Moreover, the novelty of polymer nanocomposites characteristics make them useful in engineering and biosensors [4,5]. They are in great demand across industries because of their exceptional mechanical, thermal, electrical, and barrier qualities [6,7].

Poly(4-chloroaniline) (P(4-ClAni)) polymer has several uses due to its ability to resist high temperatures without degradation [8]. Ensuring stability and durability of device performance over time, particularly under demanding conditions, is a crucial quality for optical devices [9]. Many optical devices, which require transparent and conductive materials for improved light emission and energy efficiency, extensively utilize P(4-ClAni) polymer owing to its remarkable features [10]. The remarkable optical transparency of PCA allows reliable detection and interpretation of light devices [11]. In addition, P(4-ClAni) finds utility in organic photovoltaic (OPV) cells, where effective charge transfer is crucial for turning sunlight into power [12]. Its high thermal stability, optical transparency, and strong charge transport make it ideal for creating high-performance devices with improved functionality [13,14].

* Corresponding author: aamahmad@ju.edu.sa
https://doi.org/10.15251/DJNB.2024.192.989

Furthermore, the properties of Fe_2O_3 have led to its widespread use in composites across various sectors [15]. As a reinforcement ingredient in composites, Fe_2O_3 is suitable due to its high hardness, strength, and stiffness, among other mechanical attributes [16]. Incorporating iron oxide nanoparticles into a polymer matrix enhances the material's tensile strength, improving its mechanical properties [17]. Composites reinforced with iron oxide are thus valuable for the construction, automotive, and aerospace sectors [18]. Among Fe_2O_3 remarkable properties is its ability to resist high temperatures without deterioration, ascribed to its high melting and decomposition temperatures [19]. As a result, Fe_2O_3 is a valuable ingredient for composites used in coatings, heat-resistant materials, and aeronautical parts [20].

In the present investigation, the polymer P(4-ClAni) and the composite Fe_2O_3/P(4-ClAni) with different amounts of Fe_2O_3 were prepared using the chemical oxidative polymerization technique. The resulting samples were characterized by FTIR, SEM, XRD, and UV-Vis techniques. The optical behavior of the Fe_2O_3/P(4-ClAni) nanocomposites has been improved compared to the polymeric P(4-ClAni). The results showed that the fabricated composites could be applied to flexible electronic devices with their novel characteristics.

2. Experimental details

Nanocomposite films of poly 4-chloroaniline and poly (4-chloroaniline/Fe_2O_3) were prepared on glass using the green oxidative polymerization method [21, 22]. The procedure involves creating the poly (4-ClAni) layer on the glass sheet submerged in the solution. Distilled water and ethanol were used to rinse the films that had formed on the glass. Lastly, the films were dried overnight in a microwave set to 60°C. Moreover, utilizing the same method described for the polymerization of poly(4-ClAni), three nanocomposite films containing Fe_2O_3 were produced. The monomer and HCl solution were supplemented with ferric chloride powder at various percentages (2%, 4%, and 6%). Afterward, a homogenous solution was obtained by dissolving the $FeCl_3$ with the magnetic stirrer for two hours. The samples were labelled as the P(4-ClAni), P(4-ClAni)/Fe_2O_3-I, P(4-ClAni)/Fe_2O_3-II, and P(4-ClAni)/Fe_2O_3-III, respectively.

The XRD analyses of samples were measured with the X-ray generator using the Cu-Kα, wavelength 0.15406 nm. The FTIR spectra were determined through the FTIR spectrometer (a Bruker Alpha) via the KBr pellet technique. The SEM pictures were given via the Hitachi S-4800 operating at 30 kV. The absorbance spectra were obtained using a UV-visible spectrophotometer (Shimadzu UV-2401PC) within a 190-1100 nm wavelength range.

3. Results and discussion

The FTIR technique was employed to specify the structure and functional groups of the prepared samples. The FTIR spectra of the pure poly(4-ClAni) film and poly(4-ClAni)/Fe_2O_3 nanocomposite films with different contents of the Fe_2O_3 are displayed in Figure 1a. For the spectrum of pure poly(4-ClAni) film, it is clear that the stretching frequency of the N–H group appeared at wavenumber 3236 cm^{-1} [23]. The prominent peaks at 1566 and 1495 cm^{-1} are assigned to the quinoid and benzenoid rings [24]. Two small bands at 2987 and 2896 cm^{-1} indicate the stretching vibrations of the asymmetric and symmetric –CH bond. The presented peaks at 1292 cm^{-1} are given due to the stretching frequency of the aromatic C–N bond, while bands around 827 and 963 cm^{-1} represent the –CH bending frequency of the 1,2,4 trisubstituted aromatic rings [25].

Additionally, bands were observed at 1644 cm^{-1} (corresponding to C=O stretching vibration) and the bands at 617 and 722 cm^{-1} (attributed to the chloro group positioned ortho on the phenyl ring). With the addition of different concentrations of Fe_2O_3 nano-filler into the polymer-based nanocomposite, these spectra exhibit the same peaks as those of poly(4-ClAni). It is observed the intensity of peaks gradually decreases with increasing the weight percentage of the Fe_2O_3 nanoparticles. This effect is attributed to the enhancement of free electrons, leading to improvements in the optical properties of the studied samples. Furthermore, the insertion of the nano-filler affects peak positions, with bands initially located at 3236, 1292, 1143, 1097, 963, and 617 cm^{-1} shifting to

higher values. These changes indicate a strong interaction between poly(4-ClAni) and Fe_2O_3 nanoparticles.

The results obtained from the FTIR analysis suggest that poly(4-ClAni)/Fe_2O_3 nanocomposite films are more practical for optoelectronic applications. X-ray diffraction (XRD) analysis is commonly used to identify prepared films' structure and crystalline phase. The XRD patterns of the pure poly(4-ClAni) film, poly(4-ClAni)/Fe_2O_3-I, and poly(4-ClAni)/Fe_2O_3-III nanocomposite films are presented in Figure 1b. Two broad diffraction peaks at around 2θ = 19.08° and 25.08° in the pure poly(4-ClAni) pattern indicate low crystallinity and scattered chains between the planes [26]. Moreover, these broad peaks suggest the presence of the emeraldine salt structure with high electrical conductivity in pure poly(4-ClAni).

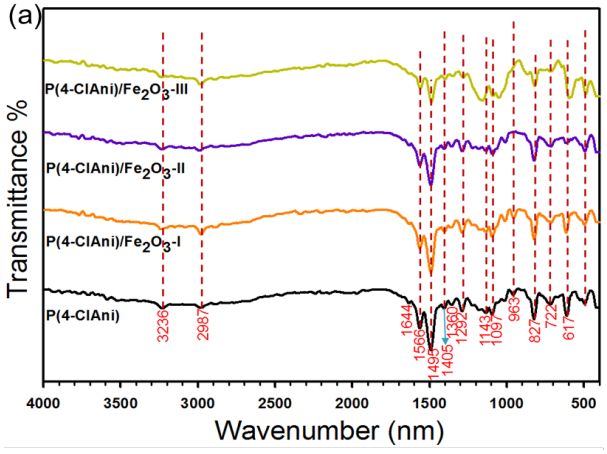

Fig. 1. (a) FTIR of P(4-ClAni) and the composite P(4-ClAni)/Fe_2O_3 films.

Variations in the XRD patterns of the poly(4-ClAni)/Fe_2O_3 nanocomposite films were observed, as depicted in Figure 1b. The peak intensity of poly(4-ClAni) increased with increasing concentrations of Fe_2O_3, indicating an increase in the crystalline nature of poly(4-ClAni) after adding Fe_2O_3 nanoparticles. Additionally, the peak at 2θ = 25.08° shifted to 2θ = 24.75° and 2θ = 24.63° as the percentage of Fe_2O_3 increased, confirming the uniform dispersion of Fe_2O_3 nanoparticles within the poly(4-ClAni) chain [27]. The characteristic diffraction bands observed at 2θ = 33.23°, 35.63°, 39.48°, 40.43°, 42.78°, 48.97°, 54.21°, 57.66°, 62.35°, 63.42°, 65.83°, 72.13°, and 75.08° are attributed to the (104), (110), (006), (113), (202), (204), (116), (108), (214), (300), (215), (1010), and (220) crystal planes of Fe_2O_3. The crystallite size (L) of Fe_2O_3 nanoparticles is given by Scherrer equation [28]:

$$L = \frac{k\,\lambda}{f\,COS\theta} \tag{1}$$

where k represents the shape factor of 0.94, f refers to the full width at half maximum, θ stands for the Bragg angle, and λ is the wavelength of the incident beam (1.54 Å). For the poly(4-ClAnil)/Fe_2O_3-III nanocomposite films, the main peak corresponding to the plane (1 1 0) was found to have Fe_2O_3 crystal sizes of approximately 13.22 nm.

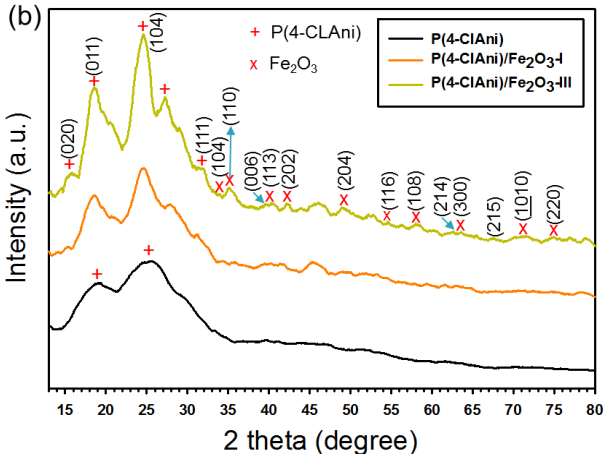

Fig. 1. (b) XRD of P(4-ClAni) and the composite P(4-ClAni)/Fe_2O_3 films.

To investigate the effect of Fe_2O_3 nanoparticles addition on the surface morphology of P(4-ClAni), SEM micrographs of P(4-ClAni) and P(4-ClAni)/Fe_2O_3 nanocomposite films containing different contents of Fe_2O_3 are presented in Figures 2(a-c). The pure P(4-ClAni) exhibits a uniform globular granular morphology with an average size of 150–225 nm, indicative of spherical morphology formed due to the convolution of many polymer chains. Upon insertion of nanoparticles into the polymer matrix, significant changes in surface morphology are observed [29]. The shape of particles varies from spherical to lamellar, and the surface morphology displays irregular plates resembling layered structures with increasing concentrations of Fe_2O_3 nanoparticles. These changes may be attributed to side chains in the aniline molecules, which restrict the linear growth of the polymer [30].

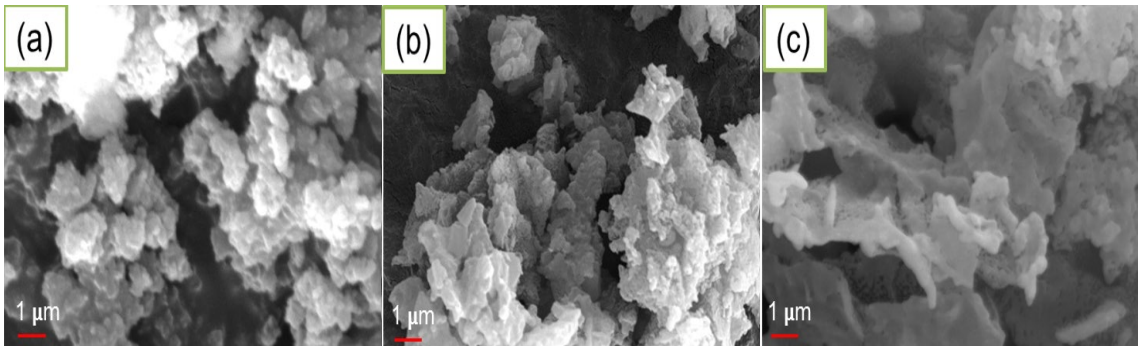

Fig. 2. SEM of (a) P(4-ClAni), (b) P(4-ClAni)/Fe_2O_3-I, and (c) P(4-ClAni)/Fe_2O_3-III.

The absorbance values of films composed of pure P(4-ClAni) and P(4-ClAni)/Fe_2O_3 with varying amounts of Fe_2O_3 are depicted in Figure 3. All samples exhibited similar absorption patterns. Increasing Fe_2O_3 content from 2.0% to 6.0% resulted in more intense absorption peaks, as observed in Figure 3. This behavior is attributed to Fe_2O_3 ability to influence the coordination links between Fe_2O_3 and P(4-ClAni) [31]. Furthermore, Figure 3 demonstrates that all sheets exhibit an absorption band likely caused by electronic transitions. Incorporating Fe_2O_3 into P(4-ClAni) enhanced these bands' intensity and improved absorbance values by acting as scattering centers. This finding is supported by EDX results, indicating compatibility between P(4-ClAni) chains and Fe_2O_3. The optical characteristics of P(4-ClAni) can be effectively controlled by adding Fe_2O_3 nanoparticles, as suggested by this research [32]. When an electron or anion transitions from the highest point of the valence band to the conduction band, it causes the absorbance band of the P(4-ClAni) spectra to

appear in the ultraviolet (UV) spectrum. The adding Fe_2O_3NPs to the P(4-ClAni) film significantly increased absorbance and the appearance of noticeable absorption bands.

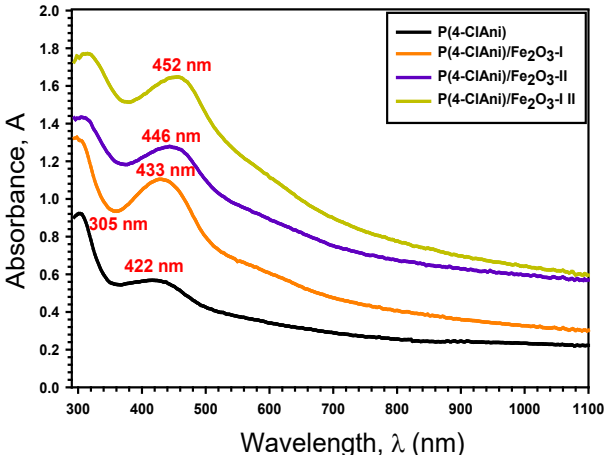

Fig. 3. The absorbance A with wavelength λ, for P(4-ClAni) and P(4-ClAni)/Fe_2O_3.

The coefficient (α) is determined by [33]:

$$\alpha = \frac{2.303\ A}{d} \tag{2}$$

Raising the concentration of Fe_2O_3 is increase the P(4-ClAni) absorbance coefficients [34]. The E_e values for the P(4-ClAni) and P(4-ClAni)/Fe_2O_3 absorption edges are shown in Figure 4. The P(4-ClAni) absorption edge is reduced from 2.88 eV to 2.35 eV, 1.62 eV, and 1.18 eV with 2%, 4%, and 6% Fe_2O_3 additions, respectively, as shown in Table 1. The change in the absorption edge of the P(4-ClAni)/Fe_2O_3 composites shows that the optical band gap of P(4-ClAni) may be fine-tuned with a relatively small amount of Fe_2O_3 nanofiller. We analyzed the sample redshift of the absorption edge and determined that the Fe_2O_3 nanofiller was bound to P(4-ClAni). Evaluations of the absorption coefficient revealed a quantifiable impact of doping P(4-ClAni) with metal oxide Fe_2O_3. Upon the addition of Fe_2O_3, the absorption coefficient values of the suggested composites are shifted to the lower energy region. This shift provides valuable insights into the electronic transitions of the molecules involved caused by electron excitation in the visible range. Additionally, the presence of P(4-ClAni)/Fe_2O_3 nanoparticles caused the absorption edge to move to the lower energy side, indicating a reduction in the optical band gap of the P(4-ClAni) polymer film [35].

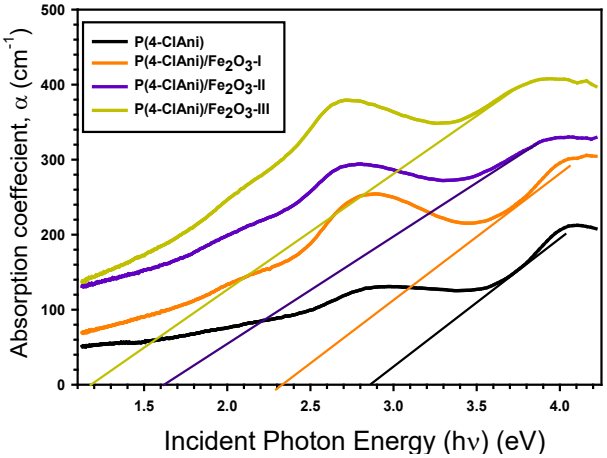

Fig. 4. Coefficient (α) with photon energy (hν) for P(4-ClAni) and P(4-ClAni)/Fe_2O_3.

The optical bandgap E_g for P(4-ClAni) and P(4-ClAni)/Fe_2O_3 is calculated using Tauc's equation [37]:

$$\alpha h\nu = A\,(h\nu - E_g)^m \tag{3}$$

Figure 5 plots the band gap and photon energy ($h\nu$). The band gap energy of P(4-ClAni) decreases from 3.57 eV to 3.39 eV, 3.07 eV, and 2.84 eV, respectively, when Fe_2O_3 is introduced at concentrations of 2.0%, 4.0%, and 6.0%. This reduction in band gap is attributed to the charge carrier of Fe_2O_3. The observed reduction in particle size suggests favorable miscibility between Fe_2O_3 and P(4-ClAni) chains. Based on these findings, composites have reached a stage where they can be utilized in optical devices, with the optical gap shrinking due to the charge-transfer complex [35]. The absorption of ultraviolet light by the P(4-ClAni)/Fe_2O_3 band occurs due to electron or anion pairs moving from the upper valence band to the conduction band. Changing or enhancing the physical characteristics of P(4-ClAni) polymer is significantly influenced by changes in its band gap caused by doping with Fe_2O_3 nanoparticles. Introducing nanofiller into a polymer matrix creates introductory forbidden-band localized states, which may affect the final Fermi level. These states serve as sites for recombination and trapping and are fundamental components of nanocomposites. Using the following formula [38], the carbon number (N) can be determined from the optical gap E_g by:

$$E_g = 34.4/N \tag{4}$$

where E_g stands for the band gap and N for the carbon cluster. Increasing the Fe_2O_3 concentration from 2.0% to 6.0% increased the N/m* values from 92 for P(4-ClAni) to 102, 125, and 146, respectively, as indicated in Table 1. This increase in nitrogen content and the resulting decrease in band gap are outcomes of the enhancements made to these composites. Changes in the matrix's crystallinity lead to shifts in the films' band gaps, influencing the bonds between the matrix and nanofiller. Additionally, a visual examination revealed a color change from completely transparent P(4-ClAni) to semi-transparent P(4-ClAni)/Fe_2O_3. Meaningful light absorption across a wide range of wavelengths was observed in the manufactured samples, resulting in nanocomposite coatings with effective ultraviolet light absorption capabilities. The figure illustrates that the band edge of the P(4-ClAni) polymer film decreases when nanoparticles are introduced into the film structure. Insulating polymers, being clear and free of contaminants or fillers, have filled valence bands and vacant conduction bands, which means they do not absorb visible light. However, due to the insulator's large band gap, injected impurities typically occupy an intermediate level, allowing absorption of visible light frequencies when electrons move from the donor plane to the conducting level.

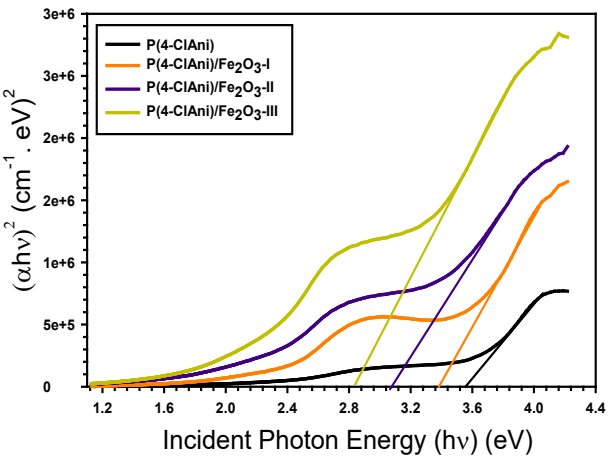

Fig. 5. The band gap E_g with photon energy for P(4-ClAni) and P(4-ClAni)/Fe_2O_3.

The Urbach energy, which represents the tail portion of the weak-photon energy area or expanded bands states, is given by [39]:

$$\alpha(\nu) = \alpha_o \, e^{h\nu/E_u} \quad (5)$$

Figure 6 illustrates the band tail of P(4-ClAni) and P(4-ClAni)/Fe_2O_3 by plotting ln (α) against photon energy. The band tail energy (E_u) of P(4-ClAni) and P(4-ClAni)/Fe_2O_3 can be determined from the opposite slope of the linear components, as shown in Table 1. With the addition of 2.0%, 4.0%, and 6.0% Fe_2O_3 to P(4-ClAni), the Urbach tail of P(4-ClAni) increased from 0.96 eV to 1.65 eV, 1.73 eV, and 1.86 eV, respectively. The increase in disorder explains why Urbach tail values increased with increasing Fe_2O_3 concentration [40]. Fluctuations in band gap energy and band tail indicate that adding Fe_2O_3 nanofiller to pure P(4-ClAni) may alter its energy states. Introducing nanofiller into a polymer matrix creates introductory forbidden-band localized states, which may influence the final Fermi level. These states are crucial for the optical properties of nanocomposites, as they act as centers for recombination and trapping. The incorporation of Fe_2O_3 nanoparticles renders P(4-ClAni) sensitive, as evidenced by the increase in the absorption coefficient. Fluctuations in band gap energy and band tail indicate the adding Fe_2O_3 to P(4-ClAni) may alter its energy states. Based on these findings, the P(4-ClAni)/Fe_2O_3 films are now better suited for use in optoelectronics devices due to their improved optical properties.

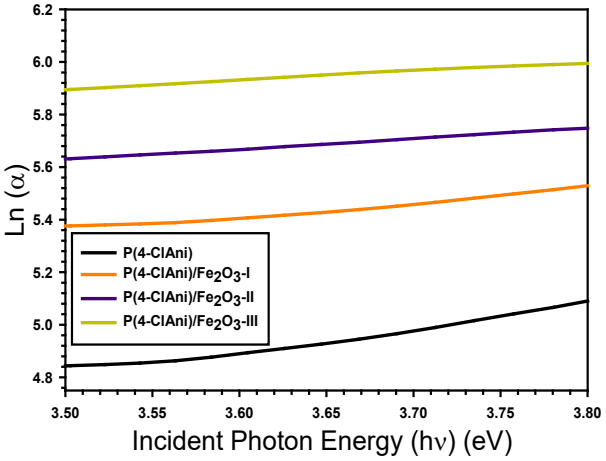

Fig. 6. Ln (α) with photon energy for P(4-ClAni) and P(4-ClAni)/Fe_2O_3.

Table 1. E_e, E_u , N and E_g for P(4-ClAni) and P(4-ClAni)/Fe_2O_3.

	Absorption edge energy (E_e, eV)	Band gap (E_g, eV)	Urbach tail (E_U, eV)	Carbon clusters (N)
P(4-ClAni)	2.88	3.57	0.96	92
P(4-ClAni)/Fe_2O_3-I	2.35	3.39	1.65	102
P(4-ClAni)/Fe_2O_3-II	1.62	3.07	1.73	125
P(4-ClAni)/Fe_2O_3-III	1.185	2.84	1.86	146

4. Conclusion

The green synthesis polymerization process was used to successfully make the nanocomposite P(4-ClAni)/Fe_2O_3 films. Analyses using XRD, SEM, and FTIR confirm the production of P(4-ClAni)/Fe_2O_3 composites. This composition was determined by EDX as 28.55% carbon, 50% oxygen, and 20% titanium. The FTIR band intensities is reduced and shifting by

incorporated Fe_2O_3 nanoparticles on P(4-ClAni). The optical absorbance was found to be greatly increased by introduction Fe_2O_3 to the P(4-ClAni). The energy gap is reduced as a result of these homo-polar interactions and defects. The band gap narrows from 3.57 eV for P(4-ClAni) to 2.84 eV, the absorption edge changes from 2.88 eV for P(4-ClAni) to 1.18 eV for P(4-ClAni)/Fe_2O_3. The findings of this study suggest that modifications to the optical performance of P(4-ClAni)/Fe_2O_3 composite films could be used in flexible electronic devices.

Acknowledgements

This research project was funded by the Deanship of Scientific Research, Princess Nourah bint Abdulrahman University, through the Program of Research Project Funding After Publication, grant No (44- PRFA-P-13).

References

[1] A Atta, H Negm, E Abdeltwab, M Rabia, M M Abdelhamied, Polymers for Advanced Technologies 34 1633 (2023); https://doi.org/10.1002/pat.5997

[2] B M Alotaibi, M R Atta, E Abdeltwab, A Atta, M M Abdelhamied Surface Innovations 12 84 (2023); https://doi.org/10.1680/jsuin.22.01078

[3] N A Althubiti, A Atta, N Al-Harbi, R K Sendi, M M Abdelhamied, Optical and Quantum Electronics 55 348 (2024); https://doi.org/10.1007/s11082-023-04600-7

[4] N A Althubiti, N Al-Harbi, R K Sendi, A Atta, A M Henaish Inorganics 1174 (2023).

[5] I A Alhagri, T F Qahtan, M O Farea, A N Al-Hakimi, S M Al-Hazmy, S E S Saeed, A E Albadri Polymers 15 384 (2023); https://doi.org/10.3390/polym15020384

[6] M A Morsi, M Abdelaziz, A H Oraby, I Mokhles) Journal of Physics and Chemistry of Solids 125 103 (2019); https://doi.org/10.1016/j.jpcs.2018.10.009

[7] A E Tarabiah, H A Alhadlaq, Z M Alaizeri, A A Ahmed, G M Asnag, M Ahamed Journal of Polymer Research 29 167 (2022); https://doi.org/10.1007/s10965-022-03011-8

[8] O Yalçın, R Coşkun, M Okutan, M Oncan, G Yeşilot Journal of Materials Science: Materials in Electronics 34 1608 (2023); https://doi.org/10.1007/s10854-023-10915-8

[9] B Gholami, M Mohammadikish, M Niakan ACS Applied Nano Materials 6 2864 (2023); https://doi.org/10.1021/acsanm.2c05254

[10] M N Ahmad, R Fakher, N Faisal, F Tahir, N A Muhammad, H Tajamal, H Sajjad, B Madeeha, KH Hamad, S Khurram Chemistry Central Journal 12 1 (2018).

[11] M Rabia, A M Elsayed, M A Alnuwaiser Processes 11 2375 (2023); https://doi.org/10.3390/pr11082375

[12] K A A Al-Ola, M Alhasani, F M Alkhatib, S O Alzahrani, K M Alkhamis, H A Katouah, M N El-Metwaly Journal of Water Process Engineering 56 104521 (2023); https://doi.org/10.1016/j.jwpe.2023.104521

[13] M M Abdelhamied, A Atta, B M Alotaibi, N Al-Harbi, A M A Henaish, M Rabia Inorganic Chemistry Communications 157 111245 (2023); https://doi.org/10.1016/j.inoche.2023.111245

[14] M M Atta, A M Abdelhamied, A M Abdelreheem, M R Berber Polymers 13 1225 (2021); https://doi.org/10.3390/polym13081225

[15] A Badawi, S S Alharthi, M G Althobaiti, A N Alharbi Journal of Vinyl and Additive Technology 28 235 (2022); https://doi.org/10.1002/vnl.21889

[16] A Badawi, M G Althobaiti, S S Alharthi, A N Alharbi, A A Alkathiri, S E Alomairy Applied Physics A 128 123 (2022); https://doi.org/10.1007/s00339-021-05154-9

[17] A A Alrehaili, A F Gharib, A El Askary, M A El-Morsy, N S Awwad, H A Ibrahium, A A Menazea Optical Materials 129 112497 (2022); https://doi.org/10.1016/j.optmat.2022.112497

[18] A A Menazea, H A Ibrahium, N S Awwad, M E Moustapha, M O Farea, M A Bajaber Journal of Materials Research and Technology 18 2273 (2022); https://doi.org/10.1016/j.jmrt.2022.03.058

[19] V Kumar, M N Alam, S S Park Journal of Polymer Research, 29 251 (2022); https://doi.org/10.1007/s10965-022-03084-5

[20] S J Kashyap, R Sankannavar, G M Madhu Materials Chemistry and Physics 286 126118 (2022); https://doi.org/10.1016/j.matchemphys.2022.126118

[21] S Iqbal, S Nadeem, M N Ahmad, M Javed, H O Alsaab, N S Awwad, A Mohyuddin Frontiers in Materials 9 874735 (2022); https://doi.org/10.3389/fmats.2022.874735

[22] M Alruqi, M Rabia, A M Elsayed, H A Hanafi, M Shaban, M M Abdel Hamied Journal of Applied Polymer Science 140 e53833 (2023); https://doi.org/10.1002/app.53833

[23] G Ravi Kumar, J Vivekanandan, A Mahudeswaran, P S Vijayanand Iranian Polymer Journal, 22 923 (2013); https://doi.org/10.1007/s13726-013-0191-x

[24] P Linganathan, J Sundararajan, J M Samuel Journal of Composites 2014 9 (2014); https://doi.org/10.1155/2014/838975

[25] K A A Al-Ola, M Alhasani, F M Alkhatib, S O Alzahrani, K M Alkhamis, H A Katouah, N M El-Metwaly Journal of Water Process Engineering 56 104521 (2023); https://doi.org/10.1016/j.jwpe.2023.104521

[26] M N Ahmad, M Ul Hassan, M Masood, F Nawaz, M N Anjum, S Z Iqbal, T Hussain, M F Farid GLOBAL NEST JOURNAL 24 53 (2022).

[27] P Linganathan, J Sundararajan, J M Samuel Journal of Composites 2014; https://doi.org/10.1155/2014/838975

[28] A A Manda, K Elsayed, M B Ibrahim, S A Haladu, F Ercan, E Çevik, Q A Drmosh Arabian Journal for Science and Engineering 48 7635 (2023); https://doi.org/10.1007/s13369-022-07462-5

[29] T Abdullah, S I Shamsah, I A Shaaban, M Akhtar, S Yousaf Synthetic Metals 299 117472 (2023); https://doi.org/10.1016/j.synthmet.2023.117472

[30] M M Abdelhamied, Y Gao, X Li, W Liu Applied Physics A 128 57 (2022); https://doi.org/10.1007/s00339-021-05189-y

[31] M M Abdelhamied, A Atta, A m Abdelreheem, A T M Farag, M M El Okr Journal of Materials Science: Materials in Electronics 31 22629 (2020); https://doi.org/10.1007/s10854-020-04774-w

[32] M Sayed, J A Khan, L A Shah, N S Shah, F Shah, H M Khan, H Arandiyan Journal of Physical Chemistry C 122 406 (2018); https://doi.org/10.1021/acs.jpcc.7b09169

[33] M A El-Sheikh, A Al-Enezy, F El-Enezy, D Ashammri, W Alrowili Egyptian Journal of Chemistry 63 8 (2020).

[34] A. El-Saftawy, S. Abd El Aal, Z. Badawy, B. Soliman Surface and Coatings Technology 253 249 (2014); https://doi.org/10.1016/j.surfcoat.2014.05.048

[35] D Sahoo, P Priyadarshini, R Dandela, D Alagarasan, R Ganesan, S Varadharajaperumal, R Naik RSC Advances 11 16015 (2021).; https://doi.org/10.1039/D1RA02368C

[36] J Sun, C H Shen, J Guo, H Guo, Y F Yin, X J Xu, X J Wen Journal of Colloid and Interface Science 588 19 (2021); https://doi.org/10.1016/j.jcis.2020.12.043

[37] M F Zaki, A M Ali, R M Amin Journal of Adhesion Science and Technology 31 1314 (2017); https://doi.org/10.1080/01694243.2016.1255455

[38] T Taha, A Saleh Applied Physics A 124 600 (2018); https://doi.org/10.1007/s00339-018-2026-2

[39] S A Kakil, B N Sabr, L S Hana, T A H Abbas, S Y Hussin Journal of the Korean Physical Society 72 561 (2018); https://doi.org/10.3938/jkps.72.561
[40] Z A Alrowaili, T A Taha, K S El-Nasser, H Donya Journal of Inorganic and Organometallic Polymers and Materials 31 3101 (2021); https://doi.org/10.1007/s10904-021-01995-2